

INTERNATIONAL SOCIETY FOR SOIL MECHANICS AND GEOTECHNICAL ENGINEERING



This paper was downloaded from the Online Library of the International Society for Soil Mechanics and Geotechnical Engineering (ISSMGE). The library is available here:

<https://www.issmge.org/publications/online-library>

This is an open-access database that archives thousands of papers published under the Auspices of the ISSMGE and maintained by the Innovation and Development Committee of ISSMGE.

The paper was published in the proceedings of the 10th European Conference on Numerical Methods in Geotechnical Engineering and was edited by Lidija Zdravkovic, Stavroula Kontoe, Aikaterini Tsiampousi and David Taborda. The conference was held from June 26th to June 28th 2023 at the Imperial College London, United Kingdom.

To see the complete list of papers in the proceedings visit the link below:

<https://issmge.org/files/NUMGE2023-Preface.pdf>

Undrained effective stress safety analysis

G. Grimstad¹, I. J. Arnesen², B. Bull³, D. Dadras-Ajirlou¹

¹*Department of Civil and Environmental Engineering, Norwegian University of Science and Technology, Trondheim, Norway*

²*Rambøll, Trondheim, Norway*

³*Multiconsult, Oslo, Norway*

ABSTRACT: The main goal of this work is to examine the short-term stability and robustness of natural slopes on an effective stress basis. This may be done using Janbu's dilatancy parameter, D , to control the effective stress path for undrained loading from the initial (static equilibrium) stress condition towards the Coulomb criterion. The concept has previously been implemented in a limit equilibrium program to do an ESAU (Effective Stress Analysis Undrained) for slopes. This work revisits the ESAU concept, now applied in finite element analyses using a hardening elastoplastic Mohr-Coulomb model with the D parameter and a strength reduction scheme. However, as indicated by Potts and Zdravkovic, the definition of safety considering a strength reduction scheme is not that straightforward with an elastoplastic hardening model. ESAU is applied to a case study of a failed natural slope and to a hypothetical natural slope.

Keywords: Slope stability; Undrained; Finite Element Analysis; Limit Equilibrium

1 INTRODUCTION

The robustness of natural (consolidated existing) slopes may be evaluated using limit equilibrium analysis under the drained condition. However, if the material in a slope under failure is expected to behave undrained, and the trigger is unknown, an undrained effective stress analysis of the slope might be considered. This is to evaluate the robustness of safety margin of the slope. Svanø and Nordal (1987) used ESAU (Effective Stress Analysis Undrained) in limit equilibrium analyses using the method of slices to calculate the Factor of Safety (FOS). In ESAU Janbus's Dilatancy parameter, D , is essential to control the effective stress path, and hence the undrained shear strength.

Janbu's Dilatancy parameter is given under an undrained (constant volume) test as:

$$D = \frac{dp}{dq} \quad (1)$$

where dp is the change in mean effective stress and dq is the change in deviatoric stress. A negative D means contractive behaviour and a positive D dilative behaviour. D is used to control the effective stress path and hence the undrained shear strength. In an ESAU approach, the undrained shear strength will always be larger than the initial equilibrium shear stress condition. Because natural (existing) slopes are standing (FOS > 1), an undrained analysis is not about short-term stability, like typical view about undrained FOS evaluations,

but about how robust the slope is for small unknown changes.

In Norway the 'direct approach' (named taken from Baker et al. (1993)) is mostly used for undrained stability of natural slopes. Direct approach in this context, means undrained analyses where the undrained shear strength is directly specified. Such analyses are, in the simplest condition, sometimes referred to as a total stress analyses (or zero friction ($\phi = 0$) analyses, typically given with coordinate dependent 'cohesion', $c = c(x,y,z) = c_u$). The considered undrained shear strength (c_u or s_u) profiles are typically established based on experience, CPT correlations and sample testing. The total stress approach requires an extensive effort in establishing the variation of the undrained shear strength in the slope. The complication is that the undrained shear strength not only depends on the effective stress and the Over Consolidation Ratio (OCR), but also on the shear direction (Aamodt et al. 2021). In addition, there is a high potential for disturbance of samples taken in the field and hence the strength parameters obtained in laboratory testing may not be relevant. In more sophisticated methods the undrained shear strength is calculated based on the effective stress conditions and material parameters (e.g., ϕ , elastic stiffness, \mathbf{D} , and hardening, H , which controls the effective stress path) together with the state parameters / internal variables (e.g., pre-consolidation stress p_c) at each point in the ground and then used in the direct approach. However, this could be viewed as an unnecessary step, as the effective stress-based model could be used under the constant volume condition directly. At first glance, one might also think

that these will be equivalent, but this is not necessarily the case for models with internal (state) variables. In a total stress approach gravity loading and material strength reduction will produce the same FOS. This is not the general case for effective stress analyses, particularly not in the drained condition, but not for the undrained condition either.

The importance of correctly estimating the robustness of natural slopes against small disturbances was demonstrated recent case study in the municipality of Gjerdrum, Norway (Grimstad et al. 2022), where a slide in soft sensitive (contractive) clay (Quick clay), under a retrogressive slide action, resulted in 10 casualties. In total 1.35 million cubic meters of quick clay was released. The cause of the slide was a small erosion in the small stream in the ravine terrain several hundred meters away from the houses, making the condition for the slope on the verge of unstable. It is the challenging condition of all these types of natural slopes in the marine clay in Norway which makes the undrained safety/stability evaluation of slopes particularly relevant. It is important to have a consistent way to evaluate the robustness of slopes involving quick clay, such that necessary measures, to an appropriate extent, is taken (cost/benefit considered). There are mapped 2300 zones of quick clay in Norway, and it is not feasible to fully stabilize all these areas with the EC7 requirement of the calculated deterministic factor of safety using a total stress approach.

2 AN ISOTROPIC HARDENING COULOMBIAN MODEL FOR ESAU

This study uses a simple variant of the isotropic hardening Drucker Prager (DP) model to incorporate the dilatancy parameter and a perfectly plastic Lode angle dependent DP ('Coulomb') model for failure.

2.1 Formulation

The isotropic elastic behaviour is here simply controlled by a constant bulk stiffness, K , and constant shear stiffness, G .

The conical-shaped yield surface of the DP model in general stress space, given as F_1 :

$$F_1 = q - M_\rho \cdot (p + a) = 0 \quad (2)$$

Where: p is the mean effective stress and q is the deviatoric stress, M_ρ is the frictional coefficient that here evolves linearly plastic straining (hardening rule, equation (3)), a is the attraction ($a = c \cdot \cot\phi$).

$$M_\rho = M_{\rho 0} + \frac{H}{p+a} (\Delta - \Delta_0) \quad (3)$$

Where: $d\Delta = d\varepsilon_{q,1}^p$, $M_{\rho 0}$ is the initial mobilized value of M_ρ .

The potential surface is given by:

$$Q_1 = q - M_\psi \cdot p - C = 0 \quad (4)$$

Where: M_ψ is the dilatancy coefficient that is a function of, H , K , D and M_ρ .

Failure is introduced through a second yield and a second potential surface:

$$F_2 = q - M^* \cdot (p + a) = 0 \quad (5)$$

$$Q_2 = q - C = 0 \quad (6)$$

Where: $M^* = M(\phi, \theta)$, here the Coulomb criterion is used for giving M^* . θ is the Lode angle.

2.2 Strength Reduction and dilatancy

The starting point of the strength reduction procedure for a hardening model is the consistency condition (Potts and Zdravkovic 2012):

$$\frac{\partial F_1}{\partial \sigma} \cdot d\sigma + \frac{\partial F_1}{\partial M_\rho} \cdot \frac{dM_\rho}{d\lambda_1} \cdot d\lambda_1 + \frac{\partial F_1}{\partial SRF} dSRF = 0 \quad (7)$$

where SRF is the *Strength Reduction Factor* and $d\lambda_1$ is the plastic multiplier for the first yield surface. The first yield surface, F_1 , is now written, considering SRF , as:

$$F_1 = q - \frac{M_\rho}{SRF} \cdot (p + a) = 0 \quad (8)$$

Using equation (7) and (8), considering an undrained triaxial test gives:

$$dq + \frac{q}{SRF} \cdot dSRF - \frac{M_\rho}{SRF} \cdot dp = \frac{H}{SRF} d\lambda_1 \quad (9)$$

We now introduce $\bar{q} = SRF \cdot q$, with the differential:

$$d\bar{q} = SRF \cdot dq + q \cdot dSRF \quad (10)$$

The interpretation of \bar{q} is the upscaled deviatoric stress given for a certain SRF . So SRF is equal to the ratio between the current equilibrium deviatoric stress, q , and the hypothetical (scaled) deviatoric stress at undrained failure \bar{q} . This resembles a total stress analysis, but without having the ultimate undrained shear strength $q_u = 2c_u$ as an input.

Now, we find the M_ψ for an undrained triaxial condition. Using (10), equation (9) simplifies to:

$$d\bar{q} - M_\rho \cdot dp = H \cdot d\lambda_1 \quad (11)$$

Using a modified form of Janbu's dilatancy relation, $d\bar{q} = dp / D$, gives:

$$\left(\frac{1}{D} - M_\rho \right) \cdot \frac{dp}{d\lambda_1} = H \quad (12)$$

Since $d\varepsilon_p^e = -d\varepsilon_p^p \rightarrow \frac{dp}{d\lambda_1} = M_\psi K$ in undrained condition, then:

$$M_\psi = \frac{D}{1 - M_\rho \cdot D} \cdot \frac{H}{K} \quad (13)$$

We see that M_ψ in equation (13) is independent of SRF . We also see that it captures the shear-induced excess water pore pressure due to the potential change in q during the stress redistribution with the same description of dilation as used during loading (change in q for $dSRF = 0$). In other words, the shear-induced excess pore water pressure will consistently develop during the strength reduction procedure under stress redistribution. However, the calculated SRF for as system (even without any stress redistribution during the strength reduction procedure) will be different to the FOS computed in a direct analysis. This has two reasons: (I) Figure 1 demonstrates that the effect of that the strength is given by $M = M(\sin\phi)$ and that the failure criterion uses $\tan\phi/SRF$ in triaxial compression (a) is quite small, but in a plane strain problem (b), the difference is larger.

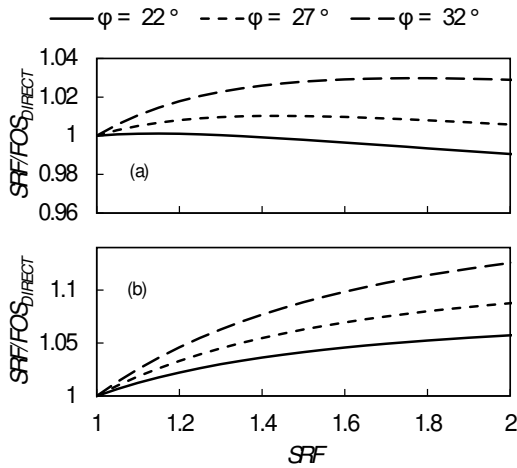


Figure 1. Ratio of SRF/FOS_{DIRECT} for Coulomb as function of SRF in triaxial compression (a), in plane strain (b).

(II) In the direct analysis $FOS = q_u / q$ which is equal to the ratio $M \cdot p / q$ giving:

$$FOS = \frac{\frac{1}{M} - D}{\frac{1}{M} - D} \quad (14)$$

Where $M_{\rho 0}$ here is the mobilization before undrained shearing. During a strength reduction procedure, the change in p (by D) is scaled for \bar{q} (and not q) which gives an additional Δp using equation (13). In addition, there is a contribution to Δp coming from geometrical “scaling” (in $p-q$) by SRF . Combined, this gives a quite complicated relationship between FOS and SRF and is dependent on the initial mobilization, the friction angle and SRF . In conclusion: in a boundary value problem, we expect different calculated FOS from this approach compared to the direct approach, because of the effect of shear-induced excess pore water pressure generated by the stress redistribution under the strength reduction procedure, the effect (I) of $\tan\phi/SRF$ to $M(\sin\phi)$ and the effect (II) of “scaling”.

2.3 Parameter limits

From equation (14) we see that $D \leq 1 / M$ for not having $FOS \rightarrow \infty$ under undrained loading. The other limits indicating $M_\psi \leq M$, is found from the second law of thermodynamics, ensuring positive dissipation for positive D . Turing around equation (13), we find the range for M_ρ (for $SRF = 1.0$):

$$\frac{1}{2D} - \sqrt{\frac{1}{4D^2} - \frac{H}{K}} \leq M_\rho \leq \frac{1}{2D} + \sqrt{\frac{1}{4D^2} - \frac{H}{K}} \quad (15)$$

This gives that the initial mobilization $M_{\rho 0}$ (for $SRF = 1.0$ and positive D) should be larger than the left side, giving:

$$M_{\rho 0} (D > 0) \geq \frac{1}{2D} - \sqrt{\frac{1}{4D^2} - \frac{H}{K}} \quad (16)$$

And that D should be limited by:

$$D \leq \frac{1}{M_\rho} \cdot \frac{1}{1 + \frac{SRF}{M_\rho^2} \cdot \frac{H}{K}} \quad (17)$$

From the above equation, we could observe that scaling H by SRF could make sense, which will also change equation (13), i.e. scaling the dilatancy by SRF .

2.4 Implementation

The model is implemented using a rather simple scheme, where the plastic multipliers $\Delta\lambda_1$ and $\Delta\lambda_2$ are calculated from the system of equations given in Equation (18), which takes into account that for the step

reaching failure, both yield surfaces will result in plastic strains.

$$\begin{bmatrix} F_1 \\ F_2 \end{bmatrix} = \Xi \cdot \begin{bmatrix} \Delta\lambda_1 \\ \Delta\lambda_2 \end{bmatrix}$$

$$\Xi = \begin{bmatrix} \left(3G + \frac{M_\rho}{SRF} \cdot M_\psi \cdot K + \frac{H}{SRF} \right) & 3G \cdot H_1 H_2 \\ \left(3G + M^* \cdot M_\psi \cdot K \right) \cdot H_2 H_1 & 3G \end{bmatrix} \quad (18)$$

Where $H_i(\Delta\lambda_i)$ is the Heaviside function and $M^* = M(\varphi, \theta, SRF)$. Finally, $\Delta\lambda_i = \max(\Delta\lambda_i, 0)$ when converged, $\sum F_i H_i < tol$.

3 VERIFICATION

First to check the procedure a homogeneous triaxial test is modelled where no redistribution takes place. The material is initially anisotropically consolidated to a given uniform mobilization ($K_0 = 0.50$). The result for compression tests with varying D is then compared to a strength reduction procedure with varying D . The parameters are given in Table 1.

Table 1. Material parameters

| G [kPa] | K [kPa] | H [kPa] | a [kPa] | $\sin\varphi$ [-] | D [-] |
|--------------|--------------|--------------|--------------|----------------------|--------------------------|
| 2000 | 4000 | 2000 | 0.1 | 0.454 | [0.5, 0.0, -1.0, -10] |

Figure 2 gives the simulated results in p - q space of the different analyses where points are given at the end of either strength reduction (at constant q) or for loading at failure under loading (for $SRF = 1$). We observe that the undrained shearing reproduces the input D when compared to the inclination of the effective stress path. The obtained failure SRF for $D = 0$ is 1.442 while the $FOS_{DIRECT} = 1.429$, giving a ratio of 1.009, which is consistent with Figure 1 (a) for $\varphi = 27^\circ$. The additional Δp produced under strength reduction, qualitatively, is as expected (the additional Δp is indicated in the figure for the different D). For $D = -1.0$ the calculated failure $SRF = 1.182$ while $FOS_{DIRECT} = 1.209$, giving a ratio of 0.978. For $D = -10$, the calculated failure $SRF = 1.021$ and $FOS_{DIRECT} = 1.040$, giving a ratio of 0.982. For $D = 0.5$, failure $SRF = 2.140$ and $FOS_{DIRECT} = 1.991$, a ratio of 1.075. Hence, we observe some un-conservatism for positive D and conservatism for negative D . This is similar to other findings, e.g. Tschuchnigg et al. (2015) using ‘B approach’, that for positive dilatancy, scaling of dilatancy by SRF will give a lower factor of safety than keeping constant dilatancy (in that case in drained condition).

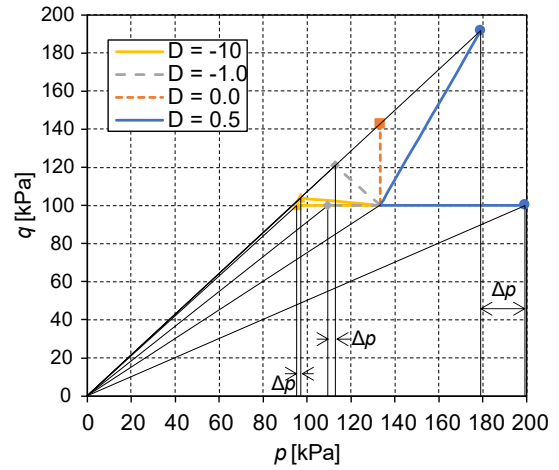


Figure 2. Simulated triaxial compression tests for different values of D .

4 CASE STUDY OF A FAILED NATURAL SLOPE

Eriksson and Arnesen (2022) used several cases of failed slopes to study for which value of D they would get $FOS = 1.0$ (failure). One of these cases is given here.

In 2012 a quick clay slide happened at Esp at Byneset, Trondheim. The initial stress condition is generated by using the Mohr-Coulomb model in the finite element code PLAXIS using parameters in Table 2 for the quick clay, for the non-quick clay φ is set to 30° . For dry crust φ is set to 35° , and K and G are increased by a factor of 3.0. The initial equilibrium condition is established by first using a K_0 procedure with K_0 of 0.50 for the clays and 0.426 for the dry crust, the groundwater is modelled as hydrostatic from the phreatic line. Following the K_0 procedure, a drained step (nil-step) is used to establish an equilibrium condition. Figure 3 gives the geometry of the Esp case.

Table 2. Material parameters, Esp

| G [MPa] | K [MPa] | H [MPa] | a [kPa] | φ [$^\circ$] | D [-] | γ [kN/m 3] |
|--------------|--------------|--------------|--------------|---------------------------|---------|--------------------------|
| 3.8 | 8.3 | 3.8 | 0.0 | 27 | 0.55 | 18.0 |
| → | | | | | | -1.0 |

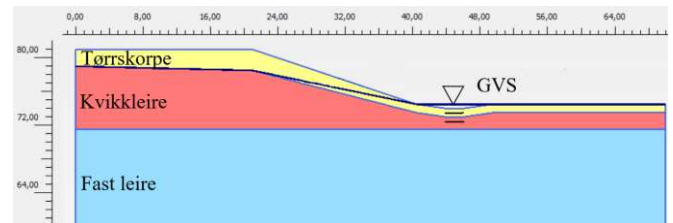


Figure 3. The soil profile and slope geometry for Esp case (Eriksson and Arnesen 2022)

The procedure is varying D , starting with $D = 0.55$ and reducing it gradually until $SRF = 1.0$ at failure. The critical value of D under undrained safety analysis is found, see Table 3.

Table 3. Results for Esp case

| $D =$ | 0.55 | 0.43 | 0.0 | -0.1 | -0.25 | -0.5 | -1.0 |
|---------|------|------|------|------|-------|------|------|
| $F.$ | 1.14 | 1.11 | 1.05 | 1.04 | 1.03 | 1.01 | 1.00 |
| $SRF =$ | | | | | | | |

It is observed that a critical value for D is around -1.0. In comparison, the drained factor of safety is calculated as 1.19 (and is independent of D). At Esp, the triggering mechanism causing the slide is not known and the SRF at failure is already quite low for $D = 0.0$. According to the national guidelines for stability in natural slopes with brittle clays (NVE 2020), the required minimum FOS for the drained analysis is $1.25 > 1.19$. Accordingly, this slope would anyway be identified as critical. Di Biagio (2020) found using direct analysis that less than approx. $3 \text{ m}^3/\text{m}$ of soil should be eroded at the toe to make the slope fail while the FOS_{DIRECT} (by gravity loading) was 1.034 before the assumed erosion (equivalent to $D \approx -0.25$). Di Biagio used the NGI-ADPSOft model (Grimstad and Jostad 2012), a model that includes strain softening, which is expected to give somewhat lower FOS than a perfectly plastic model. However, Di Biagio concluded that the calculated FOS (by gravity loading) is not that sensitive to the degree of softening. This is likely due to that there is limited redistribution under gravity loading, which is very different to cases where loading (embankment) or unloading (erosion) takes place to trigger the failure. The Esp case shows a quite consistent finding regarding safety analyses of an undrained effective stress approach versus a total stress approach.

5 UNDRAINED STABILITY EVALUATION OF A HYPOTHETICAL NATURAL SLOPE

The Esp case had a calculated drained FOS of 1.19 which is less than the requirement of 1.25 and would have anyway found to be critical. For cases where drained FOS is calculated to be higher than 1.25 an undrained stability analysis using the direct (total stress) approach should be carried out and the required min. FOS is 1.20. If FOS_{DIRECT} is less than 1.20 then improvement measures should be taken, even though the calculated drained FOS is higher than 1.25. It is common in area assessment that the drained stability is documented to be well above the requirement, but that the undrained total stress analyses give values below the threshold, thereby results in need of mitigation measures. The mitigation measures come both with economical costs and the mitigation works themselves have associated risks.

A reasonable question to ask is: What is the maximum possible calculated drained FOS when undrained

$FOS = 1.0$? If we assume that the undrained shear strength can never be below the shear stress given by Jaky's formula ($K_0^{NC} = 1 - \sin\phi$) and $a = 0$, we get the following factor, Fac , between max possible ratio of FOS for $D = 0$ (like drained without redistribution), to minimum undrained FOS of 1.0 (i.e. when $D \rightarrow -\infty$):

$$Fac = \frac{\tan \phi}{\tan \left(\arcsin \frac{1 - K_0^{NC}}{1 + K_0^{NC}} \right)} = \frac{\tan \phi}{\tan \left(\arcsin \frac{\sin \phi}{2 - \sin \phi} \right)} \quad (19)$$

Figure 4 shows the resulting limit (Fac) together with FOS lines for different K_0 as a function of ϕ and the simulation with $D = 0.0$ and $K_0 = 0.50$ in the verification test. The Esp case sits well below the "Jaky limit".

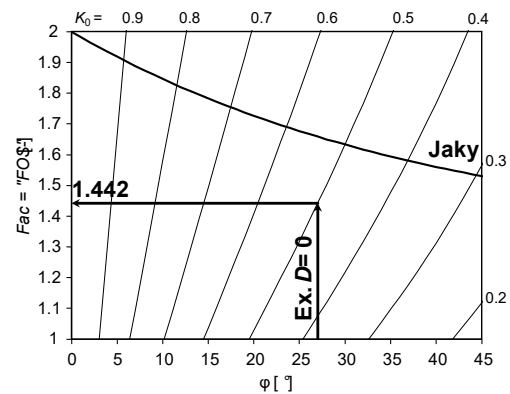


Figure 4. Visualization of equation (19) with results from the verification simulation.

5.1 The hypothetical slope

To investigate the effect of the initial condition and drained safety on the undrained safety a hypothetical case was made, see Figure 5. In this case, the extent of quick clay is limited to a "pocket". Below the clay, there is a permeable layer with hydraulic conductivity 100 times that of the clay and the quick clay. At the top, there is a 2 m layer of dry crust. Pore water pressure is calculated assuming steady state condition with groundwater level at el. +20 on the left side and at el. 0 on the right side. Initial stresses are generated by first giving K_0 of 0.50 for all layers, followed by an equilibrium step.

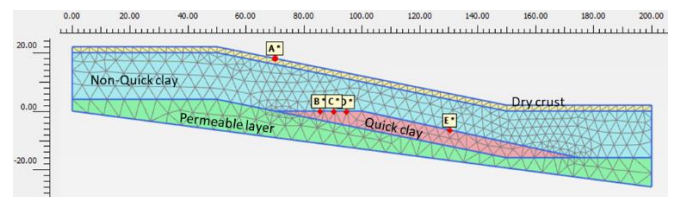


Figure 5. Hypothetical slope

Parameters for the quick lay are given in Table 1 with $D = -1.0$. For the non-quick clay, the permeable layer,

and the dry crust, $\sin\phi = 0.50$ and $D = -1.0$, $\sin\phi = 0.574$ and $D = 0$ and $\sin\phi = 0.50$ and $D = 0$ are used respectively (with the same values on the rest of the parameters as used for the quick clay). The analysis is then repeated using $K_0 = 1.0$ for initial stresses before the equilibrium step. Finally, the combination $K_0 = 1.0$ and $D = -10$ (for the quick clay) is used.

5.2 Results

For the first case, the drained FOS was calculated to be 1.63. The undrained FOS was calculated to be 1.12. The peak value of FOS_{DIRECT} (by gravity loading) was found to be 1.14. In Figure 6 the normalized effective stress paths of the stress point B-E are given (a minimum of two of these material points are within the failure mechanism for each case), $s = (\sigma_1 + \sigma_3)/2$ and $t = (\sigma_1 - \sigma_3)/2$. The contractive behaviour is observed under both loading and strength reduction. When the analysis is repeated for $K_0 = 1.0$ and $D = -1.0$, the drained FOS is the same, however, the undrained FOS now becomes 1.26 and the $FOS_{DIRECT} = 1.27$ (by gravity loading). For $D = -10$ (in the quick clay) the FOS is reduced to 1.20 by SR and to 1.21 under gravity loading.

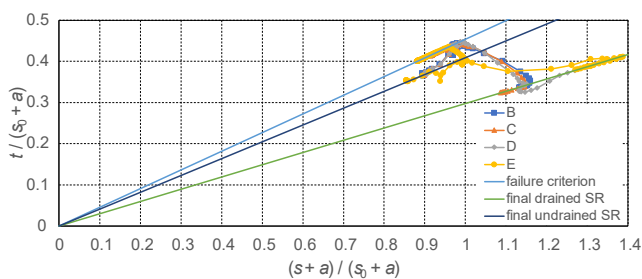


Figure 6 Normalized effective stress paths for stress points B-E under drained/undrained strength reduction or undrained gravity loading

6 CONCLUSIONS

This paper utilises the strength reduction procedure for a simple hardening model with dilatancy. In undrained conditions, the analysis considers the generation of excess pore water pressure through contraction of the material under plastic shear straining, both from the load redistribution and from the notional reduced strength. The calculated undrained FOS depends on the initial stress condition, soil strength and the dilatancy parameter D . In the case of the hypothetical slope the drained FOS was calculated to be 1.63 which is well above the criterion, while the undrained FOS was calculated to be both above and below the criterion, dependent on how the initial stresses were generated. This was different to the Esp case where both drained and undrained FOS were found to be below the respective criteria. Undrained effective stress analysis could potentially be

used to replace, or supplement, total stress analyses, especially for cases of natural slopes. In cases where a high drained FOS is calculated in combination with a low value for the calculated undrained total stress FOS , one may potentially use this for identifying unrealistic assumptions regarding either the drained analyses (e.g. pore water pressure) or regarding the input of shear strength profiles in the total stress analyses.

7 ACKNOWLEDGMENTS

Geir Svanø and Kjetil Brattlien at Bane NOR suggested this topic. Financing is provided through the Norwegian Public Road Administration (SVV), The Norwegian Water Resources and Energy Directorate (NVE) and Bane NOR (Administrator of Norwegian National Railway Infrastructure), through the SAUNA project. Arnstein Watn is acknowledged for valuable discussions.

8 REFERENCES

- Aamodt, Magnus T, Gustav Grimstad, and Steinar Nordal. 2021. "Effect of strength anisotropy on the stability of natural slopes." In *Nordic Geotechnical Meeting*, 012025. Helsinki: IOP Publishing.
- Baker, R., S. Frydman, and M. Talesnick. 1993. 'Slope stability analysis for undrained loading conditions', *International Journal for Numerical and Analytical Methods in Geomechanics*, 17: 15-43.
- Di Biagio, Amanda Johansen. 2020. 'Numerisk modellering av erosjonsutløste kvikkleireskred'.
- Eriksson, Brede Bull, and Ivar Jevne Arnesen. 2022. 'Udrenerte effektivspenningsbaserte stabilitetsanalyser av naturlige skråninger', NTNU.
- Grimstad, Gustav, and Hans Petter Jostad. 2012. "Stability analyses of quick clay using FEM and an anisotropic strain softening model with internal length scale." In *NGM 2012. Proc of the 16th Nordic Geotechnical Meeting*, 675-80. Copenhagen: Danish Geotechnical Society.
- Grimstad, Gustav, Steinar Nordal, Inger-Lise Solberg, and Hanne Bratlie Ottesen. 2022. 'Om kvikkleire og skredet den 30. desember 2020 i Gjerdrum', *Naturen*, 146: 69-82.
- NVE. 2020. "Sikkerhet mot kvikkleireskred: vurdering av områdestabilitet ved arealplanlegging og utbygging i områder med kvikkleire og andre jordarter med sprøbruddegenskaper. ." In: The Norwegian Water Resources and Energy Directorate.
- Potts, D.M., and L. Zdravkovic. 2012. 'Accounting for partial material factors in numerical analysis', *Géotechnique*, 62: 1053-65.
- Svanø, G, and S Nordal. 1987. "Undrained effective stress stability analysis." In *9th European conference on soil mechanics and foundation engineering.*, 871-75. Dublin: A. A. Balkema, Rotterdam.
- Tschuchnigg, F., H. F. Schweiger, and S. W. Sloan. 2015. 'Slope stability analysis by means of finite element limit analysis and finite element strength reduction techniques. Part I: Numerical studies considering non-associated plasticity', *Computers and Geotechnics*, 70: 169-77.